ACS SENSORS

Article

Cite This: ACS Sens. 2019, 4, 2615−2622

pubs.acs.org/acssensors

Dual-Signal Readout of DNA Methylation Status Based on the Assembly of a Supersandwich Electrochemical Biosensor without Enzymatic Reaction

Qiumei Feng, Mengying Wang, Li Qin, and Po Wang*

Department of Chemistry, Jiangsu Normal University, Xuzhou 221116, China

ABSTRACT: A highly sensitive and selective biosensing system was designed to analyze DNA methylation using a dual-signal readout technique in combination with the signal amplification of supersandwich DNA structure. Through the ingenious design of target-triggered cascade of hybridization chain reaction, one target DNA could initiate the formation of supersandwich structure with multiple signal probes. As a result, one-to-multiple amplification effect was achieved, which conferred high sensitivity to target molecular recognition. Based on probe 1 labeled with ferrocene and probe 2 modified with methylene blue, the target DNA was clearly recognized by two electrochemical signals at independent potentials, which was helpful for the acquisition of more accurate detection results. Taking advantage of bisulfite conversion, the methylation status of cytosine (C) was changed to nucleic acid sequence status, which facilitated the hybridization-based detection without enzymatic reaction. Consequently, the methylated DNA was detected at the femtomolar level with satisfactory analytical parameters. The proposed system was effectively used to assess methylated DNA in human blood serum samples, illuminating the possibility of the sensing platform for applications in disease diagnosis and biochemistry research.

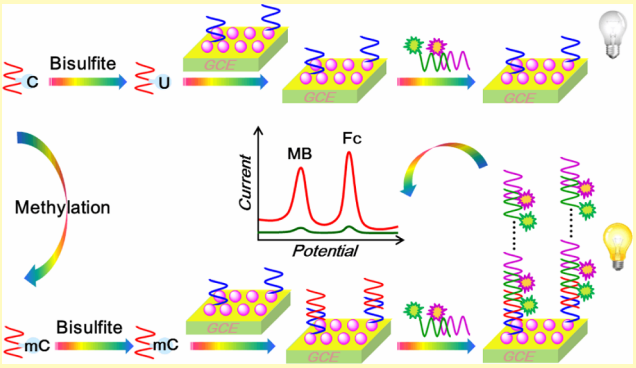

KEYWORDS: *DNA methylation, dual-signal readout, supersandwich, signal amplification, MoS_2 nanosheets*

As an important epigenetic modification of gene, DNA methylation has drawn a great deal of attention on account of its critical roles in many biological systems in mammals.[1−4] The hypermethylation of tumor suppressor gene is correlative with the loss of biological activity and the promotion of cancerous transformation.[5] It is well-known that DNA methylation is an important clinical marker for the molecular diagnostics of malignant tumor.[6,7] The recognition of DNA methylation information is helpful to make clear the underlying mechanism of genetic expression and provide a new methodology to realize early cancer diagnosis for public health.[8]

Electrochemical approaches have gained increasing interest for DNA methylation assay owing to their intrinsic properties of good portability, low instrumentation cost, simplicity, direct electronic readout, and high sensitivity and selectivity.[9−14] In 2008, Niwa's group pioneered a revolutionary methodology for the DNA methylation detection according to the direct oxidation behaviors of DNA bases.[15] In light of the electrochemical response from a nanocarbon film electrode,[15−17] DNA methylation level was efficiently monitored in a rapid and straightforward way,[15−17] while a distinct difficulty was encountered because of the influence of thymine, whose peak potential (~1.6 V in pH 5.0 acetate buffer) was close to that of 5-methylcytosine (mC). To exclude interference by thymine, we proposed an original base pairing-based subtraction approach.[18,19] However, our previous works were global assays that detected the overall levels of mC, and the identification of gene-specific methylation site was not realized, which was highly significant for biomedical research studies.[20] Interestingly, Dai et al. implemented the recognition of the CpG site of DNA utilizing the discriminative capability of *Hpa*II endonuclease.[21] *Hpa*II restriction enzyme was proved to be an elegant reagent for DNA methylation analysis,[22−25] while *Hpa*II endonuclease could only catalyze the scission of DNA at the second cytosine (C) of 5′-C<u>C</u>GG-3′ sequence without methylation.[26] Therefore, the utility of this method was restricted to the analysis of oligonucletides with 5′-C<u>C</u>GG-3′. It was rather inept for the recognition of other CpG sites,[21,27] which limited the detection targets.

At present, most of the electrochemical methods displayed only one signal response for DNA methylation profiling, which meant an individual electrochemical signal corresponding to one target. Such a solely responsive signal was readily disturbed by some factors, including instrumental efficiency and some environmental changes (such as pH, temperature, solvent polarity, salt concentration, coreactant, etc).[28,29] As a result, some false positive or negative errors could not be easily

Received: April 17, 2019
Accepted: September 11, 2019
Published: September 11, 2019

DOI: 10.1021/acssensors.9b00720
ACS Sens. 2019, 4, 2615−2622

Scheme 1. Schematic Illustration of the Dual-Signal Readout Supersandwich Electrochemical Biosensor for the Detection of Target DNA Methylation

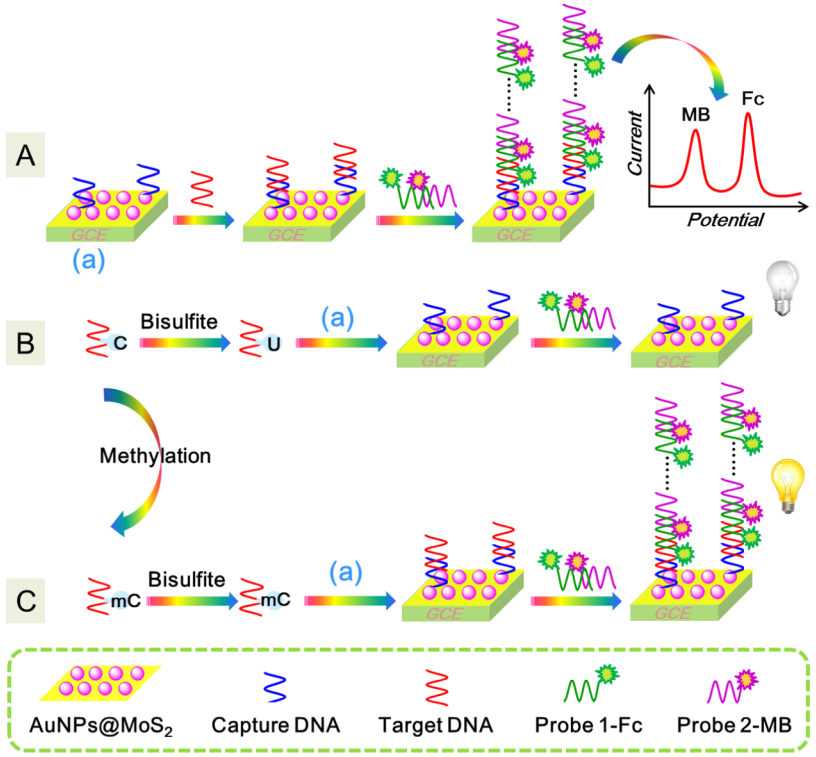

excluded from single-signal-based systems, which were often affected by ambient interferences.[30] To overcome the above shortcoming, dual-signal output biosensor, which simultaneously exhibited two signals for target analyte, paved a promising way for the acquisition of more accurate detection result. Hence, creating a dual-signal readout DNA methylation electrochemical biosensor is extremely required.

Because the amount of DNA from tumor cell is minimal in many important diagnostic scenarios, sensitivity is a significant parameter for the evaluation of the detection performance of an analytical approach. Currently, some signal amplification strategies were proposed for the analysis of DNA methylation, for instance, PCR,[31,32] rolling circle amplification (RCA),[33,34] and supersandwich DNA structure-based assembly.[35] Considering the inherent issues (including complexity, high cost, and strict experimental conditions) of PCR and RCA,[36,37] supersandwich DNA structure-based assembly was one of the most promising method.[38,39] For example, Plaxco's group pioneered an innovative supersandwich strategy for DNA assay,[40] in which each capture DNA could connect multiple signal probes through DNA hybridization. Thus, long signal concatemers were created, bringing in the effective amplification of current signal and higher sensitivity for target determination. However, the supersandwich was obtained through the hybridization event between the target molecule and signal probe with the stoichiometric relationship of 1:1. Therefore, multiple target molecules were needed for the formation of a supersandwich structure, which limited the signal amplification efficiency for the improvement of detection sensitivity.

Herein, taking advantage of the dual-signal readout technique coupled with the signal amplification of the supersandwich DNA structure, an innovative biosensing system was built to detect DNA methylation. To further enhance the sensitivity for target molecular recognition, an improved strategy was developed based on the ingenious design of target-triggered cascade of hybridization chain reaction. In this work, one target DNA could initiate the cascading hybridization reaction between two signal probes decorated with electroactive ferrocene (Fc) and methylene blue (MB), resulting in one-to-multiple amplification effect with dual-signal readout. Scheme 1 exhibits the fabrication procedure and the assay protocol of the biosensor. At first, Au nanoparticle-modified MoS_2 nanocomposites (AuNPs@MoS_2) were coated onto electrode surface via a drop-casting method, and then thiolated capture DNA probe was attached on AuNPs through Au−S linkage. Subsequently, target DNA was introduced by the partial hybridization between capture DNA fixed on electrode and one terminus of the target DNA. The other terminus of the target DNA could hybridize with a nicked probe 1-Fc and probe 2-MB nanostructure via probe 1. On account of the partial mutual hybridization between probe 1 and probe 2, long concatamers were created successfully. Eventually, by measuring both the current responses of MB and Fc, a sensitive DNA biosensor was achieved (Scheme 1A). As for the target DNA with a different methylation status, bisulfite treatment could transform C to uracil while leaving mC unchanged.[15,20] After bisulfite conversion, methylated DNA sequence can regularly hybridize with complementary capture DNA probe, while unmethylated sequence cannot be captured by DNA probe, resulting in significant signal discrimination after incubation with probe 1-Fc and probe 2-MB nanostructure (Scheme 1B,C). It should be noted that the present method is a universal technique that is not limited to the analysis of oligonucleotides with a specific sequence, and the

DOI: 10.1021/acssensors.9b00720
ACS Sens. 2019, 4, 2615−2622

Table 1. Sequences of the Oligonucleotides Used in This Study

name	sequence (5′-3′)
capture DNA	SH-TTTTCATCCAAATACTCCACACG
target DNA	CGAGTGGAAGGAAATTGCGTGTGGAGTATTTGGATGA
fully methylated target DNA	mCGAGTGGAAGGAAATTGmCGTGTGGAGTATTTGGATGA
middle hemimethylated DNA	CGAGTGGAAGGAAATTGmCGTGTGGAGTATTTGGATGA
head hemimethylated DNA	mCGAGTGGAAGGAAATTGCGTGTGGAGTATTTGGATGA
probe 1-Fc	Fc-TTTCAATTTCCTTCCACTCGTCCGGAGGAAGGTGCCG
probe 2-MB	CGAGTGGAAGGAAATTGCGGCACCTTCCTCCGGA-MB

methylation status of any CpG site can be efficiently identified without an enzymatic reaction.

EXPERIMENTAL SECTION

Chemicals and Apparatus. Molybdenum sulfide (<2 μm, 99%), polyvinylpyrrolidone (PVP), gold tetrachloride acid hydrate, $K_4[Fe(CN)_6]$, and $K_3[Fe(CN)_6]$ were provided by Sigma-Aldrich. Phosphate-buffered saline (PBS) was used as the buffer (0.1 M, pH 7.4) for all electrochemical detection. Millipore ultrapure water (18.2 MΩ cm, Milli-Q) was applied in the entire experiment. The capture DNA, probe DNA, and target DNA with different methylation status were obtained from Shanghai Sangon (China), and their sequences are shown in Table 1. Electrochemical signals including electrochemical impedance spectroscopy (EIS) were detected using a CHI660E analyzer at room temperature. The morphological characterizations of MoS_2 nanosheets and AuNPs@MoS_2 composites were observed with a JSM-6330F microanalyzer (Japan). The high-resolution transmission electron microscopy (HR-TEM) image was obtained with a Tecnai F20 TEM (FEI).

Fabrication of AuNPs@MoS_2 Nanocomposites. The MoS_2 nanosheets were prepared according to the previously reported literature with the intercalation−exfoliation method.[41,47] To synthesize AuNPs@MoS_2 nanocomposites, 100 μL of 5% PVP was introduced into 4 mL of 0.025 mg mL^{-1} MoS_2 nanosheets suspension, and then the obtained mixture was violently stirred for several minutes. Afterward, 200 μL of 10 mM $HAuCl_4$ was slowly injected. Followed by heating for 10 min at 60 °C, the color of the solution changed from brown to wine red, demonstrating the successful synthesis of AuNPs@MoS_2 nanocomposites. Finally, to purify AuNPs@MoS_2 nanocomposites, the obtained nanohybrid material was centrifuged and washed with ultrapure water.

Fabrication of the Electrochemical Biosensor. Scheme 1 displayed the preparation of the dual-signal readout supersandwich electrochemical biosensor. First, a glass carbon electrode (GCE) was used as the substrate for immobilizing AuNPs@MoS_2 nanocomposites. Before use, a cleaned GCE was pretreated with alumina powder and dried in nitrogen steam. Then, 10 μL of AuNPs@MoS_2 nanocomposites was drop cast onto the GCE surface and dried to acquire AuNPs@MoS_2/GCE. After incubation with capture DNA solution (1 μM) for 12 h in 4 °C refrigerator, the capture DNA was immobilized onto the AuNPs@MoS_2/GCE surface through the Au−S bond. Prior to assembly, the activation of capture DNA was performed in tris(2-carboxyethyl)phosphine (10 mM) to cut the S−S bond. After washing, the passivation of capture DNA/AuNPs@MoS_2/GCE was carried out in 1 mM 6-mercapto-1-hexanol (MCH) to obstruct the uncovered spots of AuNPs@MoS_2/GCE. Meanwhile, the modified capture DNA was forced to form an upright orientation, which made the latter hybridization easier.[42] Finally, the electrode was washed with the mixed solution of 1.0 mM Mg^{2+} and 20 mM pH 7.4 PBS to remove the unbounded substance and stored for the next use.

Analysis Procedure. The resultant MCH/capture DNA/AuNPs@MoS_2/GCE was submerged into 100 μL of target DNA. Before incubation, the target DNA with different methylation status were pretreated with bisulfite based on our previous work,[20] leading to the transformation of unmethylated C residues into U and the invariability of methylated ones. Then, the prepared electrode (target DNA/MCH/capture DNA/AuNPs@MoS_2/GCE) was further immersed in 100 μL of probe 1-Fc and probe 2-MB nanostructure solution for 2 h, which was gained through the hybridization of probe 1-Fc and probe 2-MB in equimolar concentration (1.0 μM). After the assembly of signal probes, an electrochemical biosensor was gained, and differential pulse voltammetry (DPV) signals were recorded in 0.1 M PBS and NaCl in nitrogen atmosphere. It was noted that the modified electrode was thoroughly washed with the mixed solution of 1.0 mM Mg^{2+} and 20 mM PBS (pH 7.4) after each assembly step.

RESULTS AND DISCUSSION

Characterizations of AuNPs@MoS_2 Nanomaterials. MoS_2, as a graphene-like layered nanomaterial, was a useful supporting substrate for decoration with noble-metal nanoparticles.[43−47] Thus, in this work, to improve the conductivity of MoS_2 nanosheets and enhance the bonding sites of capture DNA modified with SH, AuNPs were introduced onto the MoS_2 nanosheet surface. The surface morphologies of MoS_2 nanosheets and AuNPs@MoS_2 were observed with field emission scanning electron microscopy (FE-SEM). As shown in Figure 1A, the exfoliated MoS_2 nanosheets had a characteristic wrinkled layer nanostructure. After the introduction of $HAuCl_4$, many AuNPs with the size of about 12 nm grew in situ on MoS_2 nanosheets surface (Figure 1B), suggesting the formation of AuNPs@MoS_2 nanocomposites. The microscopic property of the AuNPs was studied with HR-TEM. As presented in Figure 1C, AuNPs exhibited a 0.23 nm lattice fringe spacing, which was consistent with the *d* value for

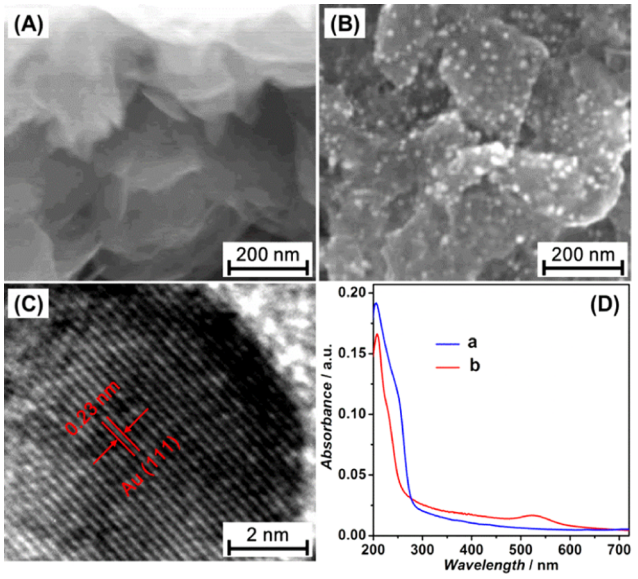

Figure 1. (A) FE-SEM image of the MoS_2 nanosheets. (B) FE-SEM image of the AuNPs@MoS_2 nanocomposites. (C) HR-TEM image of AuNPs loaded onto MoS_2 nanosheets. (D) UV−vis spectra of the MoS_2 nanosheets (a) and the AuNPs@MoS_2 nanocomposites (b).

DOI: 10.1021/acssensors.9b00720
ACS Sens. 2019, 4, 2615−2622

Au (111).[48−50] In addition, compared with the UV−vis spectrum of MoS_2 nanosheets (Figure 1D, curve a), the AuNPs@MoS_2 nanocomposites showed a new characteristic absorption centered at 520 nm (Figure 1D, curve b), attributed to the formation of AuNPs.

Electrochemical Characterization of the Sensor. EIS and cyclic voltammetry (CV) are powerful techniques for characterizing the stepwise construction process of the dual-signal readout supersandwich electrochemical biosensor. As recorded in Figure 2, in contrast to GCE (curve a), MoS_2/GCE (curve b) displayed increased resistance in EIS as well as reduced current response in CV due to the assembly of MoS_2 nanosheets with negative charges and weak conductivity. When AuNPs were decorated on MoS_2, R_{ct} of AuNPs@MoS_2/GCE (curve c) decreased obviously and the CV signal strengthened apparently compared with those of MoS_2/GCE (curve b). This phenomenon was consistent with the literature report,[51] and the results were attributed to the outstanding conductivity of the AuNPs, which greatly enhanced the interfacial charge transfer of $[Fe(CN)_6]^{3-/4-}$. Subsequently, capture DNA (curve d), MCH (curve e), methylated DNA sequence (curve f), and probe 1-Fc and probe 2-MB nanostructures (curve g) were introduced step by step, resulting in the continuous rise in R_{ct} and decrease in CV signal, which were ascribed to the nonconductivity of the DNA layer and the electrostatic repulsion between abundant negative charges of phosphate backbones and $[Fe(CN)_6]^{3-/4-}$. Thus, the electrochemical characterization witnessed the fabrication procedure of the dual-signal readout supersandwich electrochemical biosensor.

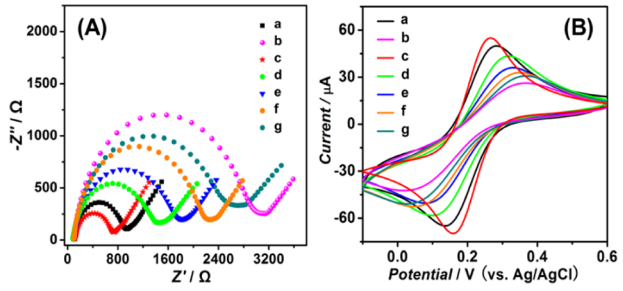

Figure 2. EIS plots (A) and CV curves (B) of different modified electrodes in 5 mM $[Fe(CN)_6]^{3-/4-}$ containing 0.1 M KCl: bare GCE (a); MoS_2/GCE (b); AuNPs@MoS_2/GCE (c); capture DNA/AuNPs@MoS_2/GCE (d); MCH/capture DNA/AuNPs@MoS_2/GCE (e); MCH/capture DNA/AuNPs@MoS_2/GCE incubated with 10 pM fully methylated target DNA (f); and (f) incubated with probe 1-Fc and probe 2-MB solution (g). EIS parameters: DC potential, 0.22 V; frequency range, 10^5−0.1 Hz; and amplitude, 0.005 V.

PAGE Analysis of the System. PAGE experiments were carried out to prove the formation of DNA long concatamers. As shown in Figure 3, lane 6 represented superhybridization products between probe 1 and probe 2. In contrast to lane 3 and lane 4, it is confirmed that probe 1 and probe 2 have been successfully hybridized and DNA long concatamers were obtained, which were consistent with reported literatures.[52−54] As anticipated, the migration rate of DNA long concatamers shifted slower after hybridization with the mixed solution of capture DNA and methylated target DNA, revealing the presence of supersandwich structures (lane 7).

Optimization of Probe Concentrations. The optimization of probe 1-Fc and probe 2-MB concentrations was carried out for the detection of 10 pM fully methylated target DNA. As presented in Figure 4, the current responses of both MB and Fc enhanced significantly with the increase in probe 1-Fc and probe 2-MB concentrations from 0.2 to 0.8 μM. Then, a stable plateau was gradually reached after 1.0 μM. Thus, the 1.0 μM concentration of probe 1-Fc and probe 2-MB was used for the following assay.

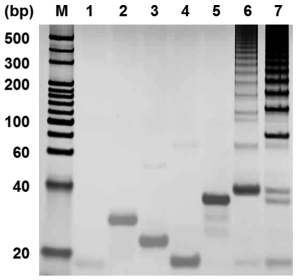

Figure 3. PAGE analysis of the system: lane M, marker; lane 1, capture DNA; lane 2, target DNA; lane 3, probe 1; lane 4, probe 2; lane 5, capture DNA + target DNA; lane 6, probe 1 + probe 2; lane 7, capture DNA + target DNA + probe 1 + probe 2.

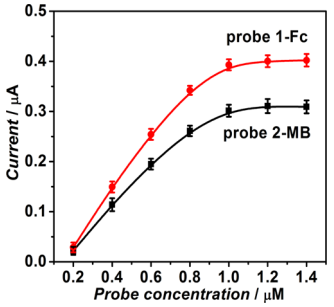

Figure 4. Optimization of probe 1-Fc and probe 2-MB concentrations for the detection of 10 pM fully methylated target DNA.

Recognition of the Methylation Information of Target DNA. The recognizing behaviors of the dual-signal readout supersandwich electrochemical system for the methylation status of target DNA were studied by detecting the current signals to different sites of methylated C. The employed target DNAs were sufficiently pretreated with bisulfite before use. As described in Figure 5, for fully methylated target DNA (curve b), the current responses of

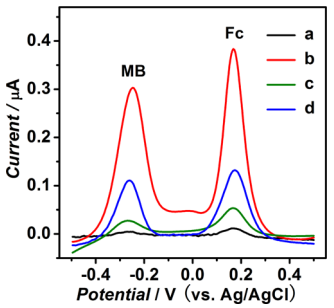

Figure 5. Background-subtracted DPV signals of the dual-signal readout supersandwich electrochemical biosensor for the hybridization of 10 pM unmethylated target DNA (a), fully methylated target DNA (b), head hemimethylated target DNA (c), and middle hemimethylated target DNA (d). DPV parameters: amplitude, 0.05 V; pulse width, 0.05 s; sampling width, 0.0167 s; and pulse period, 0.2 s.

DOI: 10.1021/acssensors.9b00720
ACS Sens. 2019, 4, 2615−2622

both MB and Fc were remarkably larger than those of unmethylated target DNA (curve a) and the hemimethylated target DNAs (curves c and d). In particular, the current signals of both MB and Fc in curve d (mC in the middle of the sequence) were stronger than those in curve c (mC in the head of the sequence), ascribed to the greater effect of the central mismatch effect on the hybridization efficiency and duplex stability. The above results also revealed that the C methylation modification exhibited almost no influence on the DNA hybridization, and our developed electrochemical biosensor could selectively discriminate the methylation position of target DNA with sequence specificity.

Analytical Applications. The sensitivity and analytical performance of the dual-signal readout supersandwich electrochemical biosensor were evaluated by the detection of various concentrations of fully methylated target DNA sequence. As demonstrated in Figure 6A, the current responses of MB and

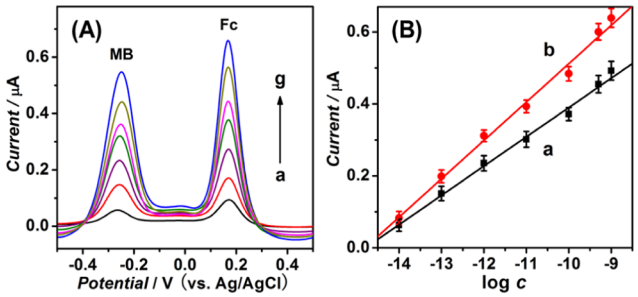

Figure 6. (A) Background-subtracted DPV signals of the dual-signal readout supersandwich electrochemical biosensor for the detection of different concentrations of methylated target DNA (a−g: 10 fM, 100 fM, 1 pM, 10 pM, 100 pM, 500 pM, and 1 nM, respectively). (B) Linear relationship between the peak current and the logarithm of the methylated target DNA concentration.

Fc increased along with the increasing of the DNA concentrations from 10 fM to 1 nM. It was revealed that both the peak current increments of MB (curve a) and Fc (curve b) were logarithmically related to the concentrations of methylated target DNA, with the correlation coefficients of 0.997 and 0.996, respectively (Figure 6B). The limit of detection (LOD) for methylated target DNA sequence reached 700 aM for MB and 450 aM for Fc. In addition, the assay precision of the biosensor was evaluated using six independent biosensors. The resulting RSD was around 4.7% for the detection of 10 pM methylated target DNA. Moreover, the detection performance of the dual-signal readout system was compared with a variety of reference methods, including SERS,[55] SPR,[56] colorimetric analysis,[57] photoelectrochemical (PEC) biosensor,[58] electrochemiluminescence (ECL),[59,60] fluorescence,[61,62] and electrochemical detection.[63−65] It was demonstrated in Table 2 that the proposed approach exhibited relatively better analytical parameters for target analysis. To confirm the validity of the detection system in a complex sample matrix, the sensing platform was challenged with the assay of the fully methylated target DNA in human blood serum samples. The recovery tests were carried out in 10% serum samples, and the results were obtained to be 105.2%, 99.5%, 102.4%, and 96.7% for the assay of 50 fM, 500 fM, 5 pM, and 50 pM concentrations of methylated target DNA, respectively. The RSD results (from 2.6 to 5.8%) were acceptable, confirming high selectivity and precision of the method for methylated target DNA detection in complex samples.

Table 2. Comparison with Other Detection Techniques in the Assay of DNA Methylation

detection technique	linear range	LOD	ref
SERS	5 pM−5 nM	3 pM	55
SPR	2 nM−50 nM	115 pM	56
colorimetric	100 fM−10 nM	93 fM	57
PEC	100 fM−1 nM	35 fM	58
ECL	20 pM−10 nM	8 pM	59
ECL	0.1 nM−30 nM	0.047 nM	60
fluorescent	1 fM−10 pM	0.8 fM	61
fluorescent	2 nM−630 nM	0.94 nM	62
electrochemical	0.5 pM−500 pM	0.17 pM	63
electrochemical	3.9 pM−500 pM	1.2 pM	64
electrochemical	1 fM−10 nM	1 fM	65
electrochemical	10 fM−1 nM	450 aM	this work

Stability and Interference. The stability of the sensing platform was tested by the periodical analysis of 10 pM fully methylated target DNA. The current signals of MB and Fc remained 96.2% and 96.7%, respectively, of the initial electrochemical responses after one week of storage in 4 °C refrigerator, and the current declines of MB and Fc were less than 7.5% after two weeks, indicating that the proposed biosensor was stable for continual operation. The effects of possible interferences on the detection of methylated DNA were tested by adding metal ions and proteins into the sensing system for analysis. The results demonstrated that common metal ions in biological samples displayed negligible interferences on the assay of 10 pM fully methylated target DNA in a 500-fold concentration (current variations <2.5%), for instance, Ca^{2+}, Na^{+}, Mg^{2+}, K^{+}, Zn^{2+}, Mn^{2+}, Co^{2+}, Cr^{3+}, and Cu^{2+}. As for the effects from proteins, it was revealed that the signal changes of both MB and Fc were less than 5% of the initial current after the introduction of 100-fold concentration of the listed proteins, including hemoglobin, myoglobin, telomerase, and thrombin, which verified the application ability of the system in physiological samples.

CONCLUSIONS

In this work, a DNA methylation biosensing system was explored for high sensitivity and specificity. The advantages of this strategy are highlighted as follows: (1) supersandwich DNA structure exhibited a strong amplification capability via one-to-multiple amplification effect between target DNA and signal probes; (2) based on the electrochemical responses of the dual-signal readout system at two independent potentials, the detection accuracy of DNA methylation was improved; and (3) bisulfite conversion was a universal analysis technique that enabled the analysis of any CpG sites without an enzymatic reaction. In addition, on account of the outstanding interfacial features of AuNPs-decorated MoS_2 nanocomposites, the charge-transfer efficiency was improved greatly and more capture DNA strands were loaded onto the sensing interface, resulting in further improvement of detection sensitivity. As a consequence, the present strategy implemented the position recognition and sensitive detection of methylated DNA sequence at a femtomolar level, which is helpful for the epigenetic evaluation and the investigation of tumorigenesis for clinical assay.

DOI: 10.1021/acssensors.9b00720
ACS Sens. 2019, 4, 2615−2622

AUTHOR INFORMATION

Corresponding Author

*E-mail: wangpo@jsnu.edu.cn.

ORCID

Po Wang: 0000-0001-6590-2169

Notes

The authors declare no competing financial interest.

ACKNOWLEDGMENTS

We are grateful to the support from NSFC (Nos 21705062 and 21675067), the PAPD, and the foundations from Xuzhou City (No. KC19161) and Jiangsu Province (Nos BE2019645 and BK20170228).

REFERENCES

(1) Wolffe, A. P.; Matzke, M. A. Epigenetics: Regulation Through Repression. *Science* **1999**, *286*, 481−486.

(2) Jones, P. A.; Baylin, S. B. The Epigenomics of Cancer. *Cell* **2007**, *128*, 683−692.

(3) Berney, M.; McGouran, J. F. Methods for Detection of Cytosine and Thymine Modifications in DNA. *Nat. Rev. Chem.* **2018**, *2*, 332−348.

(4) Jones, P. A.; Takai, D. The Role of DNA Methylation in Mammalian Epigenetics. *Science* **2001**, *293*, 1068−1070.

(5) Robertson, K. D. DNA Methylation and Human Disease. *Nat. Rev. Genet.* **2005**, *6*, 597−610.

(6) Tsutsui, M.; Matsubara, K.; Ohshiro, T.; Furuhashi, M.; Taniguchi, M.; Kawai, T. Electrical Detection of Single Methylcytosines in a DNA Oligomer. *J. Am. Chem. Soc.* **2011**, *133*, 9124−9128.

(7) Hou, P.; Ji, M. J.; Ge, C. W.; Shen, J. Y.; Li, S.; He, N. Y.; Lu, Z. H. Detection of Methylation of Human $p16^{Ink4a}$ Gene 5′-CpG Islands by Electrochemical Method Coupled with Linker-PCR. *Nucleic Acids Res.* **2003**, *31*, No. e92.

(8) Heyn, H.; Esteller, M. DNA Methylation Profiling in the Clinic: Applications and Challenges. *Nat. Rev. Genet.* **2012**, *13*, 679−692.

(9) Muren, N. B.; Barton, J. K. Electrochemical Assay for the Signal-On Detection of Human DNA Methyltransferase Activity. *J. Am. Chem. Soc.* **2013**, *135*, 16632−16640.

(10) Furst, A. L.; Muren, N. B.; Hill, M. G.; Barton, J. K. Label-Free Electrochemical Detection of Human Methyltransferase from Tumors. *Proc. Natl. Acad. Sci. U.S.A.* **2014**, *111*, 14985−14989.

(11) Wang, X. Y.; Chen, F.; Zhang, D. X.; Zhao, Y.; Wei, J.; Wang, L. H.; Song, S. P.; Fan, C. H.; Zhao, Y. X. Single Copy-Sensitive Electrochemical Assay for Circulating Methylated DNA in Clinical Samples with Ultrahigh Specificity Based on a Sequential Discrimination−Amplification Strategy. *Chem. Sci.* **2017**, *8*, 4764−4770.

(12) Wang, P.; Han, P.; Dong, L.; Miao, X. M. Direct Potential Resolution and Simultaneous Detection of Cytosine and 5-Methylcytosine based on the Construction of Polypyrrole Functionalized Graphene Nanowall Interface. *Electrochem. Commun.* **2015**, *61*, 36−39.

(13) Tanaka, K.; Tainaka, K.; Kamei, T.; Okamoto, A. Direct Labeling of 5-Methylcytosine and Its Applications. *J. Am. Chem. Soc.* **2007**, *129*, 5612−5620.

(14) Gao, F. L.; Fan, T. T.; Ou, S. S.; Wu, J.; Zhang, X.; Luo, J. J.; Li, N.; Yao, Y.; Mou, Y. F.; Liao, X. J.; Geng, D. Q. Highly Efficient Electrochemical Sensing Platform for Sensitive Detection DNA Methylation, and Methyltransferase Activity Based on Ag NPs Decorated Carbon Nanocubes. *Biosens. Bioelectron.* **2018**, *99*, 201−208.

(15) Kato, D.; Sekioka, N.; Ueda, A.; Kurita, R.; Hirono, S.; Suzuki, K.; Niwa, O. A Nanocarbon Film Electrode as a Platform for Exploring DNA Methylation. *J. Am. Chem. Soc.* **2008**, *130*, 3716−3717.

(16) Kato, D.; Goto, K.; Fujii, S.; Takatsu, A.; Hirono, S.; Niwa, O. Electrochemical DNA Methylation Detection for Enzymatically Digested CpG Oligonucleotides. *Anal. Chem.* **2011**, *83*, 7595−7599.

(17) Kurita, R.; Yanagisawa, H.; Kamata, T.; Kato, D.; Niwa, O. On-Chip Evaluation of DNA Methylation with Electrochemical Combined Bisulfite Restriction Analysis Utilizing a Carbon Film Containing a Nanocrystalline Structure. *Anal. Chem.* **2017**, *89*, 5976−5982.

(18) Wang, P.; Mai, Z. B.; Dai, Z.; Zou, X. Y. Investigation of DNA Methylation by Direct Electrocatalytic Oxidation. *Chem. Commun.* **2010**, *46*, 7781−7783.

(19) Wang, P.; Chen, H. B.; Tian, J. Y.; Dai, Z.; Zou, X. Y. Electrochemical Evaluation of DNA Methylation Level Based on the Stoichiometric Relationship Between Purine and Pyrimidine Bases. *Biosens. Bioelectron.* **2013**, *45*, 34−39.

(20) Wang, P.; Wu, H.; Dai, Z.; Zou, X. Y. Picomolar Level Profiling of the Methylation Status of the p53 Tumor Suppressor Gene by a Label-Free Electrochemical Biosensor. *Chem. Commun.* **2012**, *48*, 10754−10756.

(21) Dai, Z.; Hu, X.; Wu, H.; Zou, X. Y. A Label-Free Electrochemical Assay for Quantification of Gene-Specific Methylation in a Nucleic Acid Sequence. *Chem. Commun.* **2012**, *48*, 1769−1771.

(22) Chen, X.; Huang, J.; Zhang, S.; Mo, F.; Su, S. S.; Li, Y.; Fang, L. C.; Deng, J.; Huang, H.; Luo, Z. X.; Zheng, J. S. Electrochemical Biosensor for DNA Methylation Detection through Hybridization Chain-Amplified Reaction Coupled with a Tetrahedral DNA Nanostructure. *ACS Appl. Mater. Interfaces* **2019**, *11*, 3745−3752.

(23) Zhang, L. Q.; Wei, M.; Gao, C. Y.; Wei, W.; Zhang, Y. J.; Liu, S. Q. Label-Free Electrochemical Detection of Methyltransferase Activity and Inhibitor Screening Based on Endonuclease *Hpa*II and the Deposition of Polyaniline. *Biosens. Bioelectron.* **2015**, *73*, 188−194.

(24) Li, W.; Wu, P.; Zhang, H.; Cai, C. X. Signal Amplification of Graphene Oxide Combining with Restriction Endonuclease for Site-Specific Determination of DNA Methylation and Assay of Methyltransferase Activity. *Anal. Chem.* **2012**, *84*, 7583−7590.

(25) Liu, S. N.; Wu, P.; Li, W.; Zhang, H.; Cai, C. X. An Electrochemical Approach for Detection of DNA Methylation and Assay of the Methyltransferase Activity. *Chem. Commun.* **2011**, *47*, 2844−2846.

(26) Zhou, H.; Han, T. Q.; Wei, Q.; Zhang, S. S. Efficient Enhancement of Electrochemiluminescence from Cadmium Sulfide Quantum Dots by Glucose Oxidase Mimicking Gold Nanoparticles for Highly Sensitive Assay of Methyltransferase Activity. *Anal. Chem.* **2016**, *88*, 2976−2983.

(27) Wang, M.; Xu, Z. N.; Chen, L. J.; Yin, H. S.; Ai, S. Y. Electrochemical Immunosensing Platform for DNA Methyltransferase Activity Analysis and Inhibitor Screening. *Anal. Chem.* **2012**, *84*, 9072−9078.

(28) Han, Y. Y.; Ding, C. Q.; Zhou, J.; Tian, Y. Single Probe for Imaging and Biosensing of pH, Cu^{2+} Ions, and pH/Cu^{2+} in Live Cells with Ratiometric Fluorescence Signals. *Anal. Chem.* **2015**, *87*, 5333−5339.

(29) Shustova, N. B.; Cozzolino, A. F.; Reineke, S.; Baldo, M.; Dinca, M. Selective Turn-On Ammonia Sensing Enabled by High-Temperature Fluorescence in Metal−Organic Frameworks with Open Metal Sites. *J. Am. Chem. Soc.* **2013**, *135*, 13326−13329.

(30) Zhang, H. R.; Wu, M. S.; Xu, J. J.; Chen, H. Y. Signal-On Dual-Potential Electrochemiluminescence Based on Luminol−Gold Bifunctional Nanoparticles for Telomerase Detection. *Anal. Chem.* **2014**, *86*, 3834−3840.

(31) Burke, D. G.; Griffiths, K.; Kassir, Z.; Emslie, K. Accurate Measurement of DNA Methylation That Is Traceable to the International System of Units. *Anal. Chem.* **2009**, *81*, 7294−7301.

(32) Clark, S. J.; Statham, A.; Stirzaker, C.; Molloy, P. L.; Frommer, M. DNA Methylation: Bisulphite Modification and Analysis. *Nat. Protoc.* **2006**, *1*, 2353−2364.

(33) Bi, S.; Zhao, T. T.; Luo, B. Y.; Zhu, J. J. Hybridization Chain Reaction-Based Branched Rolling Circle Amplification for Chem-

DOI: 10.1021/acssensors.9b00720
ACS Sens. 2019, 4, 2615−2622

iluminescence Detection of DNA Methylation. *Chem. Commun.* **2013**, *49*, 6906−6908.
(34) Liu, H. M.; Luo, J.; Fang, L. C.; Huang, H.; Deng, J.; Huang, J.; Zhang, S.; Li, Y.; Zheng, J. S. An Electrochemical Strategy with Tetrahedron Rolling Circle Amplification for Ultrasensitive Detection of DNA Methylation. *Biosens. Bioelectron.* **2018**, *121*, 47−53.
(35) Li, Y.; Luo, X. E.; Yan, Z.; Zheng, J. B.; Qi, H. L. A Label-Free Supersandwich Electrogenerated Chemiluminescence Method for the Detection of DNA Methylation and Assay of the Methyltransferase Activity. *Chem. Commun.* **2013**, *49*, 3869−3871.
(36) Chen, Y.; Wang, Q.; Xu, J.; Xiang, Y.; Yuan, R.; Chai, Y. Q. A New Hybrid Signal Amplification Strategy for Ultrasensitive Electrochemical Detection of DNA Based on Enzyme-Assisted Target Recycling and DNA Supersandwich Assemblies. *Chem. Commun.* **2013**, *49*, 2052−2054.
(37) Cheng, Y. Q.; Zhang, X.; Li, Z. P.; Jiao, X. X.; Wang, Y. C.; Zhang, Y. L. Highly Sensitive Determination of microRNA Using Target-Primed and Branched Rolling-Circle Amplification. *Angew. Chem., Int. Ed.* **2009**, *48*, 3268−3272.
(38) Chen, X.; Hong, C. Y.; Lin, Y. H.; Chen, J. H.; Chen, G. N.; Yang, H. H. Enzyme-Free and Label-Free Ultrasensitive Electrochemical Detection of Human Immunodeficiency Virus DNA in Biological Samples Based on Long-Range Self-Assembled DNA Nanostructures. *Anal. Chem.* **2012**, *84*, 8277−8283.
(39) Wang, Y. H.; Huang, K. J.; Wu, X.; Ma, Y. Y.; Song, D. L.; Du, C. Y.; Chang, S. H. Ultrasensitive Supersandwich-Type Biosensor for Enzyme-Free Amplified MicroRNA Detection Based on N-Doped Graphene/Au Nanoparticles and Hemin/G-Quadruplexes. *J. Mater. Chem. B* **2018**, *6*, 2134−2142.
(40) Xia, F.; White, R. J.; Zuo, X. L.; Patterson, A.; Xiao, Y.; Kang, D.; Gong, X.; Plaxco, K. W.; Heeger, A. J. An Electrochemical Supersandwich Assay for Sensitive and Selective DNA Detection in Complex Matrices. *J. Am. Chem. Soc.* **2010**, *132*, 14346−14348.
(41) Joensen, P.; Frindt, R.; Morrison, S. R. Single-Layer MoS_2. *Mater. Res. Bull.* **1986**, *21*, 457−461.
(42) Su, S.; Zhang, C.; Yuwen, L. H.; Chao, J.; Zuo, X. L.; Liu, X. F.; Song, C. Y.; Fan, C. H.; Wang, L. H. Creating SERS Hot Spots on MoS_2 Nanosheets with in Situ Grown Gold Nanoparticles. *ACS Appl. Mater. Interfaces* **2014**, *6*, 18735−18741.
(43) Zhou, H.; Zhang, Y. Y.; Liu, J.; Xu, J. J.; Chen, H. Y. Electrochemiluminescence Resonance Energy Transfer Between CdS:Eu Nancrystals and Au Nanorods for Sensitive DNA Detection. *J. Phys. Chem. C* **2012**, *116*, 17773−17780.
(44) Su, S.; Cao, W. F.; Liu, W.; Lu, Z. W.; Zhu, D.; Chao, J.; Weng, L. X.; Wang, L. H.; Fan, C. H.; Wang, L. H. Dual-Mode Electrochemical Analysis of MicroRNA-21 Using Gold Nanoparticle-Decorated MoS_2 Nanosheet. *Biosens. Bioelectron.* **2017**, *94*, 552−559.
(45) Huang, X.; Zeng, Z. Y.; Bao, S. Y.; Wang, M. F.; Qi, X. Y.; Fan, Z. X.; Zhang, H. Solution-Phase Epitaxial Growth of Noble Metal Nanostructures on Dispersible Single-Layer Molybdenum Disulfide Nanosheets. *Nat. Commun.* **2013**, *4*, No. 1444.
(46) Su, S.; Sun, H. F.; Cao, W. F.; Chao, J.; Peng, H. Z.; Zuo, X. L.; Yuwen, L. H.; Fan, C. H.; Wang, L. H. Dual-Target Electrochemical Biosensing Based on DNA Structural Switching on Gold Nanoparticle-Decorated MoS_2 Nanosheets. *ACS Appl. Mater. Interfaces* **2016**, *8*, 6826−6833.
(47) Sreeprasad, T. S.; Nguyen, P.; Kim, N.; Berry, V. Controlled, Defect-Guided, Metal-Nanoparticle Incorporation onto MoS_2 via Chemical and Microwave Routes: Electrical, Thermal, and Structural Properties. *Nano Lett.* **2013**, *13*, 4434−4441.
(48) Miao, X. M.; Cheng, Z. Y.; Ma, H. Y.; Li, Z. B.; Xue, N.; Wang, P. Label-Free Platform for MicroRNA Detection Based on the Fluorescence Quenching of Positively Charged Gold Nanoparticles to Silver Nanoclusters. *Anal. Chem.* **2018**, *90*, 1098−1103.
(49) Wen, T.; Zhang, D. X.; Liu, J.; Zhang, H. X.; Zhang, J. Facile Synthesis of Bimetal Au−Ag Nanoparticles in a Cu(I) Boron Imidazolate Framework with Mechanochromic Properties. *Chem. Commun.* **2015**, *51*, 1353−1355.
(50) Wang, P.; Wang, M. Y.; Zhou, F. Y.; Yang, G. H.; Qu, L. L.; Miao, X. M. Development of a Paper-Based, Inexpensive, and Disposable Electrochemical Sensing Platform for Nitrite Detection. *Electrochem. Commun.* **2017**, *81*, 74−78.
(51) Shuai, H. L.; Huang, K. J.; Chen, Y. X.; Fang, L. X.; Jia, M. P. Au Nanoparticles/Hollow Molybdenum Disulfide Microcubes Based Biosensor for MicroRNA-21 Detection Coupled with Duplex-Specific Nuclease and Enzyme Signal Amplification. *Biosens. Bioelectron.* **2017**, *89*, 989−997.
(52) Li, J. Y.; Liu, S. Y.; Sun, L. Q.; Li, W.; Zhang, S. Y.; Yang, S.; Li, J.; Yang, H. H. Amplified Visualization of Protein-Specific Glycosylation in Zebrafish via Proximity-Induced Hybridization Chain Reaction. *J. Am. Chem. Soc.* **2018**, *140*, 16589−16595.
(53) Chen, Q. S.; Zhou, S. H.; Li, C. Y.; Guo, Q. P.; Yang, X. H.; Huang, J.; Liu, J. B.; Wang, K. M. DNA Supersandwich Assemblies as Artificial Receptors to Mediate Intracellular Delivery of Catalase for Efficient ROS Scavenging. *Chem. Commun.* **2019**, *55*, 4242−4245.
(54) Li, N.; Xiang, M. H.; Liu, J. W.; Tang, H.; Jiang, J. H. DNA Polymer Nanoparticles Programmed via Supersandwich Hybridization for Imaging and Therapy of Cancer Cells. *Anal. Chem.* **2018**, *90*, 12951−12958.
(55) Hu, J.; Zhang, C. Y. Single Base Extension Reaction-Based Surface Enhanced Raman Spectroscopy for DNA Methylation Assay. *Biosens. Bioelectron.* **2012**, *31*, 451−457.
(56) Huertas, C. S.; Aviñó, A.; Kurachi, C.; Piqué, A.; Sandoval, J.; Eritja, R.; Esteller, M.; Lechuga, L. M. Label-Free DNA-Methylation Detection by Direct ds-DNA Fragment Screening Using Poly-Purine Hairpins. *Biosens. Bioelectron.* **2018**, *120*, 47−54.
(57) Geng, Y.; Wu, J.; Shao, L. J.; Yan, F.; Ju, H. X. Sensitive Colorimetric Biosensing for Methylation Analysis of *p16/CDKN2* Promoter with Hyperbranched Rolling Circle Amplification. *Biosens. Bioelectron.* **2014**, *61*, 593−597.
(58) Yin, H. S.; Sun, B.; Zhou, Y. L.; Wang, M.; Xu, Z. N.; Fu, Z. L.; Ai, S. Y. A New Strategy for Methylated DNA Detection Based on Photoelectrochemical Immunosensor Using Bi_2S_3 Nanorods, Methyl Bonding Domain Protein and Anti-His Tag Antibody. *Biosens. Bioelectron.* **2014**, *51*, 103−108.
(59) Zhang, H.; Li, M. X.; Fan, M. X.; Gu, J. X.; Wu, P.; Cai, C. X. Electrochemiluminescence Signal Amplification Combined with a Conformation-Switched Hairpin DNA Probe for Determining the Methylation Level and Position in the Hsp53 Tumor Suppressor Gene. *Chem. Commun.* **2014**, *50*, 2932−2934.
(60) Jiang, W. J.; Wu, L. N.; Duan, J. L.; Yin, H. S.; Ai, S. Y. Ultrasensitive Electrochemiluminescence Immunosensor for 5-Hydroxymethylcytosine Detection Based on Fe_3O_4@SiO_2 Nanoparticles and PAMAM Dendrimers. *Biosens. Bioelectron.* **2018**, *99*, 660−666.
(61) Cao, A. P.; Zhang, C. Y. Sensitive and Label-Free DNA Methylation Detection by Ligation-Mediated Hyperbranched Rolling Circle Amplification. *Anal. Chem.* **2012**, *84*, 6199−6205.
(62) Dadmehr, M.; Hosseini, M.; Hosseinkhani, S.; Ganjali, M. R.; Sheikhnejad, R. Label Free Colorimetric and Fluorimetric Direct Detection of Methylated DNA Based on Silver Nanoclusters for Cancer Early Diagnosis. *Biosens. Bioelectron.* **2015**, *73*, 108−113.
(63) Xu, Z. N.; Yin, H. S.; Huo, L. L.; Zhou, Y. L.; Ai, S. Y. Electrochemical Immunosensor for DNA Methyltransferase Activity Assay Based on Methyl CpG-Binding Protein and Dual Gold Nanoparticle Conjugate-Based Signal Amplification. *Sens. Actuators, B* **2014**, *192*, 143−149.
(64) Povedano, E.; Valverde, A.; Montiel, V. R. V.; Pedrero, M.; Yáñez-Sedeño, P.; Barderas, R.; Segundo-Acosta, P. S.; Peláez-García, A.; Mendiola, M.; Hardisson, D.; Campuzano, S.; Pingarrón, J. M. Rapid Electrochemical Assessment of Tumor Suppressor Gene Methylations in Raw Human Serum and Tumor Cells and Tissues Using Immunomagnetic Beads and Selective DNA Hybridization. *Angew. Chem., Int. Ed.* **2018**, *57*, 8194−8198.
(65) Huang, J.; Zhang, S.; Mo, F.; Su, S. S.; Chen, X.; Li, Y.; Fang, L. C.; Huang, H.; Deng, J.; Liu, H. M.; Yang, X. L.; Zheng, J. S. An Electrochemical DNA Biosensor Analytic Technique for Identifying

DOI: 10.1021/acssensors.9b00720
ACS Sens. 2019, 4, 2615−2622

DNA Methylation Specific Sites and Quantify DNA Methylation Level. *Biosens. Bioelectron.* **2019**, *127*, 155−160.

DOI: 10.1021/acssensors.9b00720
ACS Sens. 2019, 4, 2615−2622